[47]E. Gruneisen and H. D. Erfling, Ann. Physik 38, 399 (1940).

[48]R. Curratt (private communication).

[49]E. A. Stern (private communication).

PHYSICAL REVIEW B VOLUME 2, NUMBER 6 15 SEPTEMBER 1970

Diffusivity and Isotope-Effect Measurements in Equiatomic Fe-Co†*

S. G. Fishman,‡ D. Gupta,§ and D. S. Lieberman
Department of Metallurgy and Mining Engineering, and Materials Research Laboratory, University of Illinois, Urbana-Champaign, Illinois 61801

(Received 29 December 1969)

Several radioactive isotopes of Fe and Co were simultaneously diffused into an equiatomic FeCo alloy which exhibits fcc, bcc, and CsCl-type ordered phases with decreasing temperature. Penetration profiles were obtained by standard lathe sectioning and a grinding-sectioning technique described in this paper. From lnD-versus-$1/T$ plots, activation energies of 68.5 and 55 kcal and frequency factors of 1.26 and 0.25 cm^2/sec were obtained for diffusion of Fe^{59} in the fcc and bcc phases, respectively. From similar plots, activation energies of 69.4 and 60.0 kcal and frequency factors of 1.33 and 2.00 cm^2/sec were obtained for diffusion of Co^{57} in the fcc and bcc phases of the FeCo alloy. The average isotope-effect parameters were 0.66 in the fcc phase and 0.52 in the bcc phase. Manning's theory for concentrated alloys was used to calculate correlation factors for the FeCo alloy. From these calculated values and experimentally measured isotope-effect parameters, ΔK was determined to be slightly larger in the fcc and bcc phases of the FeCo alloy than has been reported in pure Fe. The observed decrease in the isotope-effect parameter with increasing degree of order during the bcc-to-CsCl–type ordering transformation is explained in terms of an increase in atom-jump correlation with the onset of long-range order.

I. INTRODUCTION

The predominant mechanism of diffusion in cubic metals and dilute alloys has been identified as atom-vacancy interchange. Since there is a certain probability that a diffusing atom will jump back into the vacancy and cancel out the effect of the jump on mass diffusion, its motion is described by a Bardeen-Herring-type correlation.[1] The correlation factor is the fraction of atom jumps which is effective in contributing to random diffusion and is intimately related to the diffusion mechanism. In pure metals it is a simple geometric factor which has been calculated theoretically and deduced from measurements.[2] The so-called "isotope-effect" measurement is useful for determining correlation factors and distinguishing among mechanisms of diffusion. While measurements of the isotope effect in self-diffusion have been made in a number of pure metals and dilute alloys,[3,4] little work has been reported in concentrated binary alloys. Since most materials in everyday use are composed of concentrated alloys, it is important to establish the mechanisms of self-diffusion in such materials and to understand the degree and nature of correlations in these mechanisms.

The present investigation was undertaken to measure self-diffusion, correlation, and isotope effects in concentrated alloys. The previous studies in this laboratory were on self-diffusion in highly ordered near-equiatomic β-AuCd [5,6] and β-AuZn[6,7] alloys as a function of composition and temperature; pressure effects were also investigated in the latter.[6] However, no correlation studies were made in these systems. Generally, tracer diffusion and correlation effects in nondilute alloys cannot be treated as rigorously as in pure metals and dilute alloys. The approach in such cases has been limited to two idealized models: the completely random alloy and the completely ordered alloy. In random alloys, it is assumed that the vacancy exchanges with tracer atoms occur with their characteristic jump frequencies independent of the configuration of the surrounding atoms, and the correlation of the atom jumps is of the Bardeen-Herring type. Manning[8,9] has developed a simplified model for diffusion kinetics in random concentrated alloys which yields equations demonstrating the primary effects to be expected. In the case of ordered alloys, the problem can be reduced to a reasonably simple form, since the alloy may be considered to consist of two interpenetrating sublattices where each sublattice is occupied by atoms of one kind. The primary constraint on vacancy motion in the ordered lattice is the requirement of maintaining long-range order.

Three diffusion mechanisms have been proposed for atomic motion in CsCl-type ordered alloys which leave the degree of long-range order un-

changed: (i) next-nearest-neighbor jump from body center to body center, [10] (ii) divacancy mechanism,[7] and (iii) a highly correlated process with a minimum of six atom-vacancy jumps in the next-nearest-neighbor direction. [11] Wynblatt[12] concluded from his calculation of the activation energy of motion for the three proposed mechanisms (using a central-force model with a modified Morse potential) that the Huntington-Elcock-McCombie six-jump model is the most probable of the three. Gupta *et al.* [5] observed in ordered β-AuCd that D^*_{Au}/D^*_{Cd} falls within the limits predicted by Elcock's model as was also observed in β-CuZn,[13] β-AgMg,[14] and β-AuZn. [6] All of this recent work seems to support the third mechanism, although indirectly, and more direct evidence is required. The isotope-effect measurement in ordered and disordered phases could provide such direct information.

The analytical expression for the isotope-effect parameter E can be written as[15]

$$E_\beta = \frac{1 - D_\beta/D_\alpha}{1 - (m_\alpha/m_\beta)^{1/2}} \quad , \tag{1}$$

where D_α and D_β are the diffusion coefficients and m_α, m_β the masses of isotopes α and β, respectively. If only one atom changes position in the lattice but the energy of motion is shared with others during the jump, the isotope-effect parameter is defined as[16,17]

$$E_\beta \equiv f_\beta(\Delta K) \quad , \tag{2}$$

where f_β is the correlation factor defined earlier and ΔK is the fraction of the translational kinetic energy possessed by the jumping atom in the direction of the jump at the saddle point. The quantity ΔK is, thus, a measure of the coupling of the jumping atom with the rest of the crystal and corrects for the deviation of the atomic vibrational frequency from the $m^{1/2}$ dependence. [18] For a pure metal, f_β is a function only of crystal structure and diffusion mechanism, E_β is measured experimentally, and ΔK is inferred from experiment, models, and theory.

For a random binary AB alloy, where diffusion takes place by atom-vacancy jumps, the correlation is relatively small, f_β approaches unity, and the isotope-effect parameter is appreciable. In ordered alloys, if the motion of a vacancy is highly correlated, qualitatively it can be seen from (2) that $E_\beta \simeq f_\beta^n \Delta K$ (where n is the number of jumps in the correlated sequence) and thus E would be perhaps an order of magnitude smaller than for the uncorrelated case. Thus, an alloy displaying an order-disorder transformation should show a transition in the isotope-effect parameter with increasing degree of order if the diffusion mechanism is highly correlated in the ordered state.

Much of the data in concentrated binary alloys pertain to characterization of self-diffusion of both species. [4,14] Isotope-effect studies[19,20] have been made in fcc NiCr alloys and CuZn alloys. However, the latter measurement (in disordered and nearly ordered β-CuZn) remains inconclusive.

The 50-at.% FeCo alloy was particularly attractive for such studies, since it exhibits a sequence of solid-state transformations from disordered fcc to disordered bcc at 980 °C and from bcc to the ordered CsCl-type structure at 730 °C. The temperature region of the disordered phases is not unreasonable for diffusion work, but below the ordering temperature, such studies are difficult. Several radioactive tracers (Fe^{59}, Fe^{55}, Co^{57}, and Co^{60}) are fortunately available for diffusion and isotope-effect studies and it was possible to measure self-diffusion and strength of isotope effect in all three phases of the alloy, as will now be described. Hirone, Kunitomi, and Sakamoto[21] measured the diffusivity of Co^{60} in FeCo over the temperature range 840–1250 °C; their results are in substantial disagreement with the present work, as will be pointed out below. Wanin and Kohn's[22] reported values of the diffusivities of Fe^{59} and Co^{60} at their one temperature of measurement are in accord with the studies presented here.

II. EXPERIMENTAL PROCEDURE

A. Specimen Preparation

Large grained specimens of 49–50-at.% Fe, $\frac{1}{2}$ in. in diameter and 3 in. in length, were grown from 99.99%-pure Fe and 99.99%-pure Co sponge. Owing to the large range in solid solubility in these alloys, small errors in composition would not be expected to affect the measured diffusivities in the disordered phase significantly, although the effect might be more important in the ordered phase. The metals were melted, mixed, and directionally solidified in Al_2O_3 crucibles with a tapered end supported by a water-cooled Cu pedestal in an rf furnace. In this manner, grains as large as $\frac{1}{4}$ in. in diameter were obtained. Following growth, the specimens were annealed for several weeks at 950 °C, spark cut into cylinders $\frac{3}{8}$ in. in length polished with progressively finer emery paper and a 0.05-μ Al_2O_3 wheel to satisfactory smoothness and flatness, and etched in dilute NITAL to remove the cold work.

B. Diffusion Measurements

In order to determine diffusion coefficients and isotope-effect parameters, measurements of penetration of radiotracers into bulk specimens were made. Monolayers of radioactive isotopes were

used in combinations of Fe^{55} (2.9 yr, 5.9-keV x ray)/Fe^{59} (44 day, 1.3-MeV γ ray), Fe^{59}/Co^{57} (267 day, 0.122-MeV γ ray), and Co^{57}/Co^{60} (5.3 yr, 1.3-MeV γ ray). Co^{60} present as an impurity in the Fe^{59} tracer could cause error in the half-life decay correction. However, the amount of Co^{60} present in the stock solution of Fe^{59} after a period of four half-lives was low enough to remain undetectable.[23] The various tracer combinations were *simultaneously* plated on the plane ends of the specimens from a bath consisting of distilled water saturated with ammonium oxalate. After plating, the specimens were sandwiched between polished Al_2O_3 wafers which served to prevent evaporation of the isotope from the surface of the specimens and any chemical reaction between the alloy and the quartz capsule. They were then sealed off after being evacuated to 10^{-6} Torr. The diffusion anneals were carried out in resistance-wound furnaces controlled to $\pm 1\,^{\circ}C$. The furnace temperatures were read with a Pt-Pt 13%-Rh thermocouple which agreed to within $0.1\,^{\circ}C$ with one calibrated by the National Bureau of Standards.

After the diffusion anneal, a layer of at least twice the thickness of the expected diffusion distance was removed from the cylindrical surface of the specimens to eliminate surface-diffusion effects. For an instantaneous plane source diffusing in a semiinfinite crystal, the concentration N_i of the ith radiotracer is given as a function of penetration distance x by[24]

$$N_i = [W_i/(\pi D_i t)^{1/2}]\exp(-x^2/4D_i t) \quad , \qquad (3)$$

where W_i is the total amount of plated ith tracer, D_i is its diffusion coefficient, and t is the annealing time. This expression implies that a plot of $\ln N_i$ versus x^2 will be a straight line with a slope of $-1/4D_i t$. The relative concentration of two isotopes, α and β, diffusing simultaneously is thus

$$\ln(N_\alpha/N_\beta) = \text{const} + (1 - D_\beta/D_\alpha)(x^2/4D_\beta t) \; . \qquad (4)$$

Therefore, a plot of $\ln(N_\alpha/N_\beta)$ versus $x^2/4D_\beta t$ permits determination of $1 - D_\beta/D_\alpha$ which is proportional to the isotope effect [Eq. (1)]. By diffusing two tracers simultaneously, the errors arising from composition and structural variations from specimen to specimen, annealing time and temperature, and sectioning are eliminated.[5]

It was desired to take at least 8–10 sections for each penetration profile. For those specimens in which the tracer penetration was of the order of 3–5 mils, the lathe-sectioning technique, described in detail elsewhere,[13] was used. Consecutive sections were removed from the specimen parallel to the face and the chips collected and weighed. The chips for the isotope-effect measurement were dissolved in NITAL and dried to a uniform film in the planchet before counting. The uniformity of the film was controlled by slowly rotating the planchet containing the dissolved sample at a speed of 1 rpm under an infrared lamp. Care was taken to insure that the solution was evaporated slowly to avoid bubbles in the film. Specimens which were dissolved and dried several times exhibited counting fluctuations consistent with the statistics. The chips for the Fe^{59}/Co^{57} diffusivities and the Co^{57}/Co^{60} measurements were counted directly since no appreciable absorption of these radiations occurred. The distance of penetration in each case was determined from the weight of the section and the diameter and density of the sample. Typical lathe-section thicknesses were about 0.3 mils. A different sectioning technique had to be employed for small tracer penetrations at low temperatures. Sections of the order of $1\,\mu$ in thickness were obtained by a grinding apparatus constructed for this experiment rather similar to those used by other workers. A $\frac{11}{8}$-in.-diam planchet containing an adhesive-backed disc of SiC polishing paper was held in the center of a Buehler 296012S polisher. The specimen was held in contact with the polishing paper by a shaft mounted perpendicular to the plane of the wheel and offset $\frac{1}{4}$ in. from the wheel center. The shaft, which was rotated in a direction opposite to that of the wheel by a motor-belt assembly, was allowed to float freely in a cylindrical greased tube which was machined to a close tolerance so that the shaft was maintained perpendicular to the polishing wheel. The weight on the shaft was varied from 1.4 to 4 lb. Specimens to be sectioned were first mounted on the lathe and a side cut taken to eliminate effects of surface diffusion.

Whereas, in the lathe-sectioning technique, the face to be sectioned could be aligned for parallel sectioning independently of the back face, this was not the case in the grinding technique. Although the shaft recess was parallel to the polishing surface, the specimen surface to be ground would not be parallel unless both planar surfaces of the specimen were parallel. In polishing the specimens prior to plating, it was extremely difficult to get the faces sufficiently parallel. However, parallelism was achieved by turning the specimen over and grinding the back of the specimen until the planar faces were parallel. Unfortunately, the back face of the specimen was thus rendered unfit for sectioning, in contrast with the lathe technique where both faces could be plated and sectioned. The specimen face being sectioned was examined after the first complete turn of the polishing wheel to make certain that the scratches on the surface were evenly distributed over the face of the spec-

imen.

By varying the wheel speed, number of turns, paper coarseness, and weight on the shaft, sections from < 1 to ~ 8 μ in thickness were obtained. The thickness of the section was determined from the weight of the grind and the known diameter and density of the specimen. The planchet, with the polishing paper, was placed directly under the scintillation detector and the radioactive emissions counted. Due to the fineness of the ground particles, no appreciable absorption of the 5.9-keV x ray occurred. A limiting factor in the grind method was the error in the weight of the sections. A typical weight of a 1-μ section was about 1 mg. Since the microbalance used was read with a probable error of 20 μg, the weighing error approached 2% when sections of less than 1 μ in thickness were weighed. Although the planchets were stored in a desiccator prior to sectioning, some error may have been introduced due to moisture pickup during grinding. However, the diffusivities obtained by the lathe and grind techniques on the same specimen agreed to within experimental error (2%), as will be shown.

C. Counting

The selective counting of the isotopes of each given pair Fe^{55}/Fe^{59}, Co^{57}/Co^{60}, or Fe^{59}/Co^{57} was accomplished by energy discrimination using a scintillation detector with a 5-mil Be window and a 2-in.-diam 2-in.-thick NaI(Tl) crystal. Both high-energy γ rays of Fe^{59}, γ rays of Co^{57}, and the low-energy x rays of Fe^{55} could be detected and counted with the same detector. Counting successive aliquots of Fe^{59} and Fe^{55} indicated that there was no effect of count rate on the results of the determination in the range used in the experiment. During counting, the following procedures were adopted. Samples were placed in exactly the same position under the scintillation counter to avoid geometry effects. The samples were counted in a random order to avoid superposition of equipment drift. Sections which were recounted, when corrected for differences in decay time, showed fluctuations consistent with the counting statistics. Since, at most, count rates of the order of 10 000 counts/min were used, no dead-time correction was necessary. Standards were counted before and after each section and equipment drift, decay and background corrections were calculated on a computer by modifying an existing program. Corrections were also made for Compton scatter in low-energy windows as a result of high-energy radiation by counting pure standards and determining the relative amount of radiation detected in the low-energy window. At least 50 000 counts were taken for each section so that the statistical-counting uncertainty was less than 0.5%.

III. RESULTS

Penetration profiles (plots of ln specific activity versus penetration distance squared) of Fe^{55} and of Fe^{59} and Fe^{55} in equiatomic FeCo alloy are shown in Figs. 1 and 2. The profiles for diffusion anneals at temperatures of 795 °C and above were obtained with the lathe technique, and it is seen that these are linear over at least two orders of magnitude in N. The profiles for diffusion anneals at temperatures less than 795 °C were obtained with the grind technique. It was possible to obtain linearity over only about one order of magnitude, presumably due to the contribution of grain boundary and/or dislocation diffusion at the low temperatures of anneal; only the linear portions of these plots were employed in calculating the diffusion coefficients. Figure 3 shows the results using both the lathe and grind techniques on the same specimen for diffusion of Fe^{55} at 904 °K; the agreement is seen to be within experimental error. The values of the diffusion coefficients for the Fe^{59}, Fe^{55}, and Co^{57} tracers at different annealing temperatures are

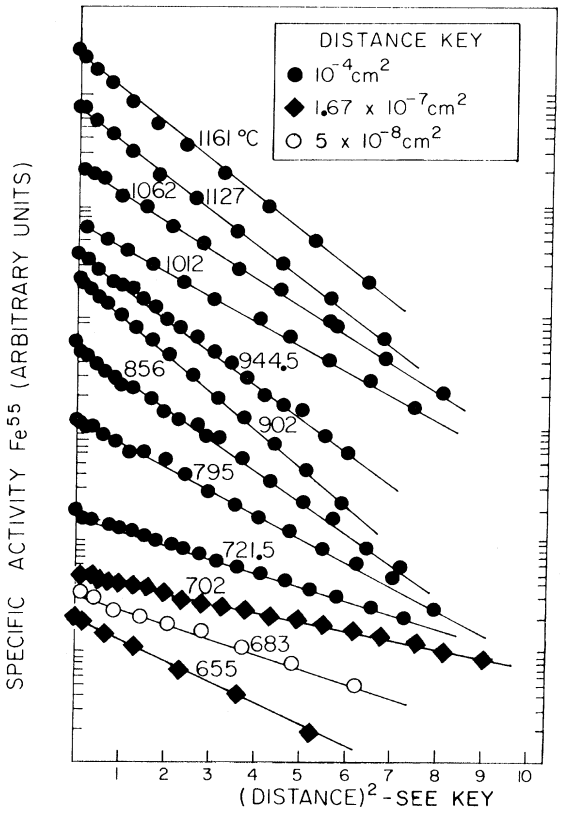

FIG. 1. Penetration profiles of Fe^{55} in FeCo.

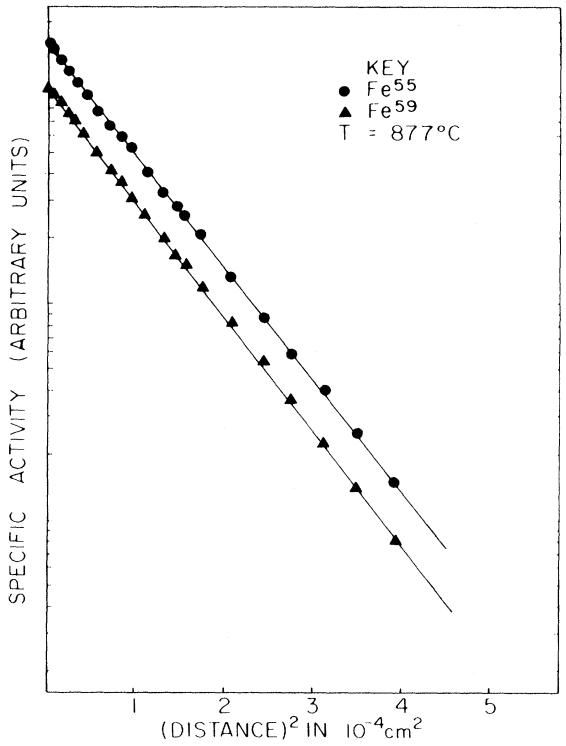

FIG. 2. Typical simultaneous penetration profiles of Fe^{59} and Fe^{55} in FeCo.

listed in Table I for the three phases. The largest source of error in values obtained with the lathe-sectioning technique is due to inaccuracy of temperature measurement (e.g., a 2 °C error at 1000 °C results in a 5% error in diffusion coefficient). Since other errors such as weight, counting, etc., were less than 2%, the total error in measurement of diffusion coefficients is estimated to be about 5%. The larger errors at lower temperatures are due to the difficulty of taking off measurable thin sections with the grinding technique.

Plots of $\ln(N_{55}/N_{59})$ versus $x^2/4D_{59}t$ over a temperature range spanning the three phases of the alloy are shown in Fig. 4; values of $1-D_{59}/D_{55}$, which are equal to the slopes in Fig. 4, are summarized in Table II. It can be seen that the slopes of these curves, which are proportional to the isotope-effect parameter, appear to be noticeably smaller below $T_c = 730$ °C in the ordered region than above this temperature in the disordered regions. The experimental values of E_{Fe} are listed in Table II and plotted as a function of temperature in the lower part of Fig. 5. The average value for E_{Fe} in the fcc phase is 0.66 ± 0.08 and in the bcc phase is 0.52 ± 0.08.

One measurement was made to determine the Co isotope-effect parameter in the fcc phase ($E_{Co} = 0.77 \pm 0.10$). Errors in the isotope-effect parameter in the ordered phase are very large as compared to those in the disordered phases, due to significant decay of the Fe^{59} tracer during the 4–6-mon diffusion anneals at the low temperatures, inadequate depth of tracer penetration even for these long anneals, and significant "short-circuit" diffusion mentioned above. Consequently, the penetration profiles for these runs are not very satisfactory and exhibit appreciable scatter; little quantitative reliance should be placed on the isotope-effect parameter in this region although there seems to be a trend toward lower values at lower temperatures.

The temperature dependence of Co^{57} and Fe^{59} diffusion coefficients in the FeCo alloy (Arrhenius plot) is shown in the upper part of Fig. 5. The behavior of $\ln D$ is distinctly different in the fcc, bcc, and CsCl-type ordered phases; the transformation temperatures in this alloy are indicated by the vertical dashed lines. The diffusion parame-

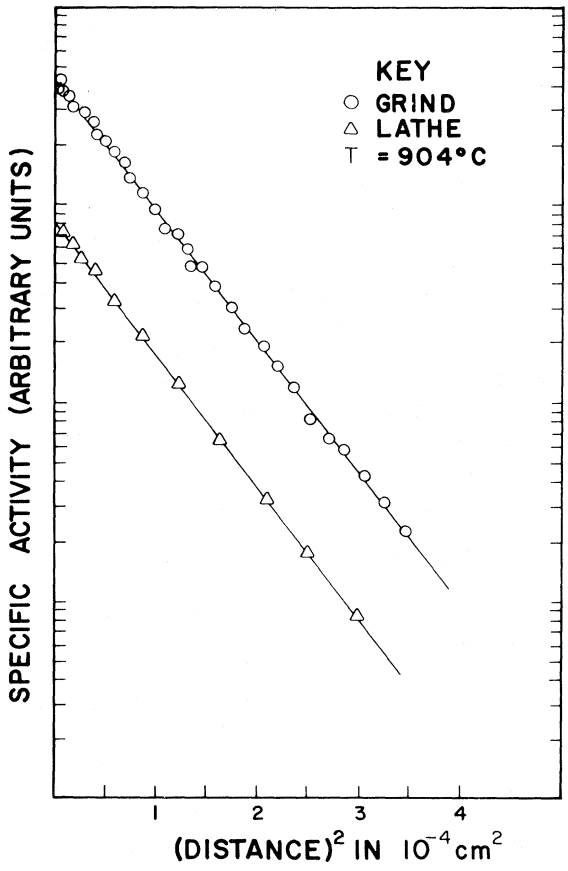

FIG. 3. Penetration profiles of Fe^{55} using the grind and lathe techniques on the same specimen.

TABLE I. Values of the diffusion coefficients for the Fe^{59}, Fe^{55} tracers in FeCo.

Temperature (°C)	Phase	$D(Fe^{59})$ (cm^2/sec)	$D(Fe^{55})$ (cm^2/sec)	$D(Co^{57})$ (cm^2/sec)	$D_{Fe^{59}}/D_{Co^{57}}$
655	CsCl-type	1.56×10^{-15}	1.56×10^{-15}		
655	CsCl-type	1.18×10^{-15}		1.15×10^{-15}	1.0
683	CsCl-type	8.72×10^{-15}	8.68×10^{-15}		
683	CsCl-type	1.02×10^{-14}		1.19×10^{-14}	0.9
702	CsCl-type	5.05×10^{-14}	4.79×10^{-14}		
704	CsCl-type	4.29×10^{-14}		3.40×10^{-14}	1.2
721.5	CsCl-type	8.72×10^{-14}	8.70×10^{-14}		
721.5	CsCl-type	1.47×10^{-13}		1.30×10^{-13}	1.1
795	bcc	1.02×10^{-12}	1.03×10^{-12}		
795	bcc	9.45×10^{-13}		8.12×10^{-13}	1.2
856	bcc	6.77×10^{-12}		5.17×10^{-12}	1.3
877	bcc	1.04×10^{-11}	1.07×10^{-11}		
887	bcc	1.34×10^{-11}		1.21×10^{-11}	1.1
902	bcc	1.80×10^{-11}	1.85×10^{-11}		
939.5	bcc	4.68×10^{-11}		3.80×10^{-11}	1.2
944.5	bcc	5.01×10^{-11}	5.12×10^{-11}		
1012	fcc	2.96×10^{-12}	3.00×10^{-12}		
1020	fcc	3.91×10^{-12}		2.63×10^{-12}	1.5
1060	fcc	•••			
1062	fcc	7.95×10^{-12}	8.14×10^{-12}	6.54×10^{-12}	
1127	fcc	2.24×10^{-11}	2.28×10^{-11}		
1129	fcc	3.70×10^{-11}		2.48×10^{-11}	1.5
1161	fcc	5.30×10^{-11}	5.34×10^{-11}		
1164	fcc	5.75×10^{-11}		4.32×10^{-11}	1.3

ters Q and D_0 are listed in Table III. The coefficients for both Co and Fe show a sharp increase associated with the fcc to bcc transformation. The resolution of the data does not warrant the drawing of separate lines for Co and Fe in the region below the ordering temperature. Attempts at interpreting unique values of Q in this region from this data are not very fruitful nor meaningful since the degree of long-range order is probably still changing (even) at the lowest temperature at which they were taken.

IV. DISCUSSION AND CONCLUSIONS

A. Diffusion of Binary Species in Equiatomic FeCo

As seen in Fig. 5, the temperature dependence of D in the fcc and bcc phases is described adequately by an Arrhenius relation. The values of Q and D_0 for the diffusion of Fe^{59} and Co^{57} in the FeCo alloy are listed in Table III. The Q and D_0 obtained for the diffusion of Fe^{59} in the equiatomic alloy are comparable to those reported for the diffusion of Fe^{59} in pure Fe: $Q = 67.9$ kcal and $D_0 = 0.49\ cm^2$/sec in the fcc phase,[25] and $Q = 60.0$ kcal and $D_0 = 2.0\ cm^2$/sec for ferromagnetic[26] Fe. The data of Wanin and Kohn[22] for the diffusivities of Fe and Co (presumably separately) in FeCo at 1200 °C have been put on Fig. 5 as described in the caption; their points lie pretty well on the lines drawn through the present data. However, Hirone, Kunitomi, and Sakamoto[21] report for the diffusion Co^{60} in 50–50-at.% FeCo 41.8 and 27.4 kcal/mol for the Q's and 1.1×10^{-4} and $2.6\ cm^2$/sec for the D_0's in the fcc and bcc regions, respectively. It is difficult to see how even "correcting" this work for the isotope effect to permit comparison with the present studies on Co^{57} will substantially improve the rather considerable disagreement with the results summarized in Table III.

The sharp rise in diffusivity for Fe^{59} and Co^{57} upon transformation from fcc to bcc in the alloy is not unexpected. This is consistent with a higher motional energy E_m, in the more close-packed fcc phase, since the energy that must be possessed by the jumping atom to reach the saddle point is higher. The change in the preexponential frequency factor ($D_0 = \gamma a^2 \bar{\nu} f e^{\Delta S/R}$, where γ is a geometric factor, a the lattice parameter, $\bar{\nu}$ a mean lattice frequency, and ΔS the entropy change associated with the process) also contributes to this rise in diffusivity with transformation from fcc to bcc phases. Since the Zener-Wert relationship[27]

$$\Delta S = \lambda \beta Q / T_m \qquad (5)$$

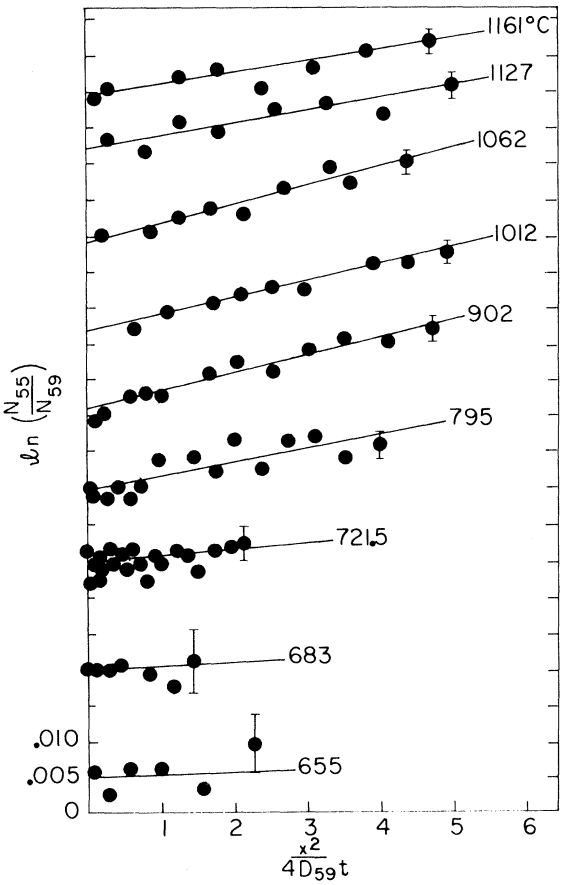

FIG. 4. Plots of relative concentrations of Fe^{59} and Fe^{55} in equiatomic FeCo.

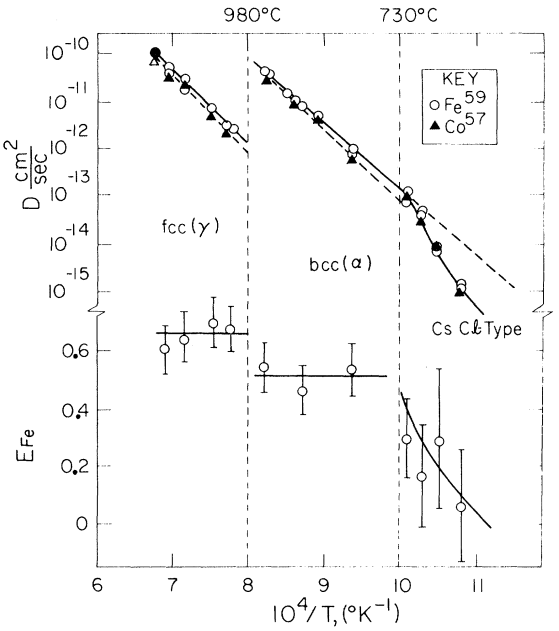

FIG. 5. Diffusivities of Fe^{59} and Co^{57} (upper) and isotope-effect parameter (lower) as a function of reciprocal temperature in the three phases of FeCo; the dashed lines indicate the transition temperatures between the phases denoted. The data of Wanin and Kohn (Ref. 22) for the diffusivity of Fe^{59} and Co^{60} in FeCo at 1200 °C is also shown as ● and Δ, respectively. Their Co^{60} point has first been "corrected" to Co^{57} using the isotope effect E of Table III; the correction of ~ 2% is hardly discernible in the fugure. Agreement with the present work is satisfactory.

TABLE II. Values of $1-D_\beta/D_\alpha$, for Fe, from the slopes in Fig. 4.

Temperature (°C)	$1-D_{59}/D_{55}$	E_{Fe}	f (Calc)
655	0.002 ± 0.020	0.06 ± 0.20	
683	0.010 ± 0.020	0.30 ± 0.20	
702	0.005 ± 0.020	0.16 ± 0.20	
721.5	0.010 ± 0.014	0.30 ± 0.15	
795	0.018 ± 0.008	0.54 ± 0.08	0.707
877	0.015 ± 0.008	0.46 ± 0.08	0.705
902	0.022 ± 0.010	0.64 ± 0.10	0.715
944.5	0.019 ± 0.008	0.55 ± 0.08	0.701
1012	0.023 ± 0.008	0.67 ± 0.08	0.745
1062	0.024 ± 0.008	0.71 ± 0.08	0.764
1127	0.022 ± 0.008	0.65 ± 0.08	0.743
1161	0.021 ± 0.008	0.61 ± 0.08	0.756
Temperature (°C)	$1-D_{60}/D_{57}$	E_{Co}	f (Calc)
1060	0.019 ± 0.008	0.773 ± 0.10	0.808

predicts that the entropy change is proportional to Q, a change in Q will also result in a change in D_0. In Eq. (5), λ is an empirical constant β is the measured temperature dependence of the elastic modulus, and T_m is the temperature of the melting point.

With the onset of long-range order, $\ln D$-versus-$1/T$ plots for Co and Fe diffusion deviate increasingly from linearity. At temperatures less than T_c, the necessity of maintaining the equilibrium degree of order places constraints on the diffusion

TABLE III. Diffusion parameters for FeCo.

Phase	Isotope	Q (kcal/mole)	D_0 (cm^2/sec)
fcc	Fe^{59}	68.5 ± 2.0	1.26 ± 0.10
fcc	Co^{57}	69.4 ± 2.0	1.33 ± 0.50
bcc	Fe^{59}	55.0 ± 1.0	0.25 ± 0.10
bcc	Co^{57}	60.0 ± 2.0	2.00 ± 0.50
CsCl	Fe^{59}, Co^{57}	133.0 ± 10.0	· · ·

process resulting in a lower diffusivity of the ordered alloy than in the disordered alloy. At temperatures only slightly lower than T_c, the degree of long-range order in FeCo is probably not high. The diffusion parameters, therefore, are expected to be strongly dependent on the increasing order and depart from a simple Arrhenius temperature dependence. The curvature in Fig. 5 in the CsCl-type phase is reminiscent of diffusion[13] in β-CuZn. As the temperature is decreased further, the degree of long-range order approaches its maximum value, unity. It is believed that a highly ordered state can be preserved during the diffusion process by the Elcock-McCombie correlated six atom-vacancy jump sequence mentioned above. Substantially lower diffusion coefficients and higher activation energies should be observed for such correlated jump sequences as the temperature of diffusion is decreased into the ordered region; this appears to be the case in Fig. 5.

It was observed that Fe diffuses about 40% faster than Co in the fcc phase and 20% faster in the bcc phase. This difference cannot be due entirely to the mass difference between the Fe and Co atoms. It is of the same order as the $D_{Fe}/D_{Co} \sim 1.3$ in both fcc and bcc Fe reported by Walter and Peterson.[28] They attributed this difference in diffusion coefficients of Fe and Co to a "repelling of vacancies" by the Co atoms. However, the ratio D_{Fe}/D_{Co} in the ordered phase of FeCo at the lowest temperature measured in this work (655 °C) is of the order unity and appreciably different from the corresponding ratios in alloys known to be highly ordered at the temperatures of diffusion. For example, in equiatomic β-AuCd, D^*_{Cd}/D^*_{Au} has been reported to be approximately 1.3. The difference in D's was attributed by Gupta *et al.*[5] to the difference between the saddle-point energies on the two sublattices. In the FeCo system, the ordering temperature is about 730 °C below the melting point (compared with the AuCd system which is believed to be ordered to the melting point) and the ordering energy may be significantly lower because of the similarity between Fe and Co atoms.

B. Isotope Effect

As mentioned above, E_{Fe} listed in Table II is expressed as the product of two terms ΔK and f_{Fe}. In concentrated alloys, f_{Fe} cannot be calculated from geometric factors alone (as in pure metals) and there is no satisfactory theory for it nor for ΔK. Manning[8,9] treated the kinetics of diffusion in a random alloy using a simplified model. He assumed that the jump frequencies w_A and w_B of tracer atoms A and B into vacancies are independent of the surrounding configuration, and that all vacancy exchanges with nontracer atoms occur with an average frequency w. These assumptions, which are not valid in a concentrated alloy, are even less so in a dilute alloy. However, this model does yield the following simple equation which predicts the main effects expected in concentrated alloys:

$$f_A = \frac{(M_0+2)(N_A D^*_A + N_B D^*_B) - 2D^*_A}{(M_0+2)(N_A D^*_A + N_B D^*_B)} \quad ; \qquad (6)$$

D^*_A, D^*_B, N_A, and N_B are the tracer diffusion coefficients and mole fractions for A and B atoms, respectively, and M_0 is a constant equal to 7.15 for fcc and 5.33 for bcc crystals.[3] The correlation factor has been studied in only a few concentrated binary systems. From their measurements of the isotope effect for Cr in Ni-rich CrNi alloys, Heumann and Reerink[19] report a value of f_{Cr} close to that predicted by Manning's theory.

1. fcc *Phase*

Using Manning's theory and known results for pure metals, certain inferences can be drawn. It is generally accepted that diffusion in fcc metals and dilute alloys occurs via atom-vacancy interchange. Since Fe and Co atoms are adjacent in the Periodic Table, and consequently very similar in size, mass, and electronic configuration (as reflected in the large range of solid solubility), it is not unreasonable to expect the diffusion behavior in FeCo alloys to be similar to that in pure Fe. In pure metals with vacancy-exchange diffusion mechanisms, ΔK is less than unity.[2] If the further assumption is made that ΔK is the same for Fe atoms as for Co atoms, then from Eq. (2)

$$E_{Fe}/E_{Co} \cong f_{Fe}/f_{Co} \quad . \qquad (7)$$

In order to test the validity of Manning's theory for this alloy, E_{Co} was also measured in an FeCo alloy (with a nominal composition of 50-at.% Fe) for Co^{60} and Co^{57} at 1060 °C. The ratio of E_{Fe}/E_{Co} was found to be 0.92 ± 0.10 as compared to a ratio of $f_{Fe}/f_{Co} = 0.95 \pm 0.05$ from Eq. (6) and experimental values of D^*_{Fe}/D^*_{Co} (Table I). This excellent agreement between the measured and calculated ratios constitutes strong evidence for the applicability of Manning's theory, at least for concentrated fcc alloys. Values of f_{Fe} calculated from Eq. (6) are listed along with experimental values of E_{Fe} in Table II. Using average values for E_{Fe} of 0.66 ± 0.10 and for f_{Fe} of 0.75 ± 0.05, ΔK was estimated to be 0.88 ± 0.10 in the fcc phase. This is consistent with the values reported for other fcc metals: $\Delta K = 0.86$ for Ag[29] and $\Delta K = 1.0$ for Pd.[30] However, a somewhat lower value of $\Delta K = 0.68$ has been reported for pure fcc Fe.[28]

2. bcc *Phase*

The mechanism of diffusion in bcc metals and dilute alloys is not as well understood as in fcc metals and dilute alloys.[31] Vacancy, divacancy, and interstitial mechanisms have all been suggested as possible in bcc metals.[31] Using an average value for E_{Fe} of 0.52 ± 0.18 from Fig. 5 and an average value for f_{Fe} of 0.70 ± 0.05 calculated from Eq. (6) (which assumes a vacancy mechanism), ΔK was determined to be 0.73 ± 0.10 in the bcc phase of the equiatomic FeCo alloy. This is somewhat higher than values in the literature for pure bcc metals. Barr and Mundy[32] reported $\Delta K = 0.50$ for Na and Walter and Peterson[28] reported $\Delta K = 0.59$ in α-Fe. In these two cases of pure metals, values of f were calculated from simple geometric factors. The larger values of ΔK obtained in the FeCo alloy (for the fcc and bcc phases) rather than in pure Fe indicate that there may be somewhat less coupling between the jumping Fe atom and lattice in the alloy.

3. *Ordered* CsCl-*Type Phase*

A plot of E_{Fe} versus reciprocal temperature for the three phases is shown in Fig. 5. The uncertainty in the values of E_{Fe} listed in Table II is larger for the ordered phases than for the other phases and is related to the difficulty in making precise diffusivity measurements at such low temperatures, particularly with the grinding device employed here. The effects of short-circuit diffusion as observed by Peterson and Rothman[33] also could cause some uncertainty in the values of E_{Fe}, especially in the low-temperature measurements. Graham[34] has reported that short-circuiting effects are responsible for the low values of E he observed in γ-Fe. In the present investigation, since the specimens were extremely large grained and linear penetration profiles were obtained, it appears that the short-circuiting effects (if any) on the measured isotope-effect parameter are negligibly small. Assuming that E is no more sensitive to short-circuiting effects than is D, E_{Fe} decreases as the temperature decreases and the corresponding degree of long-range order in the CsCl-type phases increases. As mentioned above, f lies between 0 and 1, and approaches 0 for highly correlated diffusion mechanisms. In their work in the CuZn system, Rothman and Peterson[20] suggest *a priori* that the value of ΔK may be relatively insensitive to the process of ordering. If this is true, changes measured in E_{Fe} may be attributed principally to a change in f, and consequently to a change in diffusion mechanism as the alloy becomes more highly ordered. The results of Rothman and Peterson were inconclusive due in part at least to the presence of only partial order. In this investigation it was observed that E_{Fe} changes from about 0.50 in the disordered bcc region to about 0.06 in the ordered region. If the six-jump mechanism is assumed to be operative in the ordered region, E might be expected to be on the order of $f^6(\Delta K)$ or about 0.07, in qualitative agreement with experiment.

C. Conclusions

There are several conclusions that can be drawn from the present work. The isotope-effect measurement is a useful tool to gain information about correlation effects and diffusion mechanisms in alloys. The values of the isotope-effect parameter measured in the bcc and fcc phases in the 50-50 FeCo alloy were only slightly higher than those predicted by theory. The value of E_{Fe}/E_{Co} measured in fcc FeCo is in excellent agreement with the predictions of Manning's model for a random concentrated binary alloy. The values of ΔK inferred from experiment and theory indicate a lower degree of coupling between the lattice and a jumping atom in FeCo alloys than is indicated in pure Fe. Finally, if the decrease in isotope-effect parameter in the transformation from disordered to ordered phase indicates a change from a lower to a more highly correlated diffusion mechanism, the most plausible jump mechanism in the highly ordered region is the six-jump process.

ACKNOWLEDGMENTS

The authors wish to thank the U. S. Air Force Office of Scientific Research for partial support of this work and the U. S. Atomic Energy Commission for the use of facilities in the Materials Research Laboratory of the University of Illinois, Urbana-Champaign. The continued interest and helpful comments of Dr. C. A. Wert and Dr. D. Lazarus during this investigation, the computer program developed by Dr. M. Coleman, and the careful reading of the manuscript by Dr. L. Slifkin are appreciated.

---

†Work supported in part by U. S. Air Force Office of Scientific Research under Grant No. 900-65; additional support was received from the U. S. Atomic Energy Commission through the use of technical facilities of the Materials Research Laboratory at the University of Illinois in Urbana-Champaign, Ill.

*Work based on a thesis submitted by S. G. Fishman to the University of Illinois, Urbana-Champaign, Ill., in partial fulfillment of the requirements for the degree of Doctor of Philosophy in Metallurgical Engineering.

‡Present address: U. S. Naval Weapons Laboratory, Dahlgren, Va. 22448.

§Present address: IBM Watson Research Center, Yorktown Heights, N. Y. 10598.
[1]J. Bardeen and C. Herring, *Atom Movements* (ASM, Cleveland, 1951), p. 87.
[2]K. Compaan and Y. Haven, Trans. Faraday Soc. 52, 786 (1956).
[3]N. Peterson, Solid State Phys. 22, 409 (1968).
[4]L. Barr and A. LeClair, Proc. Brit. Ceram. Soc. 1, 109 (1964).
[5]D. Gupta, D. Lazarus, and D. Lieberman, Phys. Rev. 153, 863 (1967).
[6]D. Gupta and D. Lieberman, in Proceedings of the Third Bolton Landing Conference, 1969 (unpublished).
[7]D. Gupta and D. Lieberman (unpublished).
[8]J. Manning, Acta Met. 15, 817 (1967).
[9]J. Manning, *Diffusion Kinetics for Atoms in Crystals* (Van Nostrand, New York, 1968), p. 121.
[10]P. Flinn and G. McManus, Phys. Rev. 124, 54 (1961).
[11]E. Elcock and C. McCombie, Phys. Rev. 109, 605 (1958).
[12]P. Wynblatt, Acta Met. 15, 1453 (1967).
[13]A. Kuper, D. Lazarus, J. Manning, and C. Tomizuka, Phys. Rev. 104, 1536 (1956).
[14]H. Domian and H. Aaronson, Trans. AIME 230, 44 (1964).
[15]A. Schoen, Phys. Rev. Letters 1, 138 (1958).
[16]J. Mullen, Phys. Rev. 121, 1649 (1961).
[17]A. LeClaire, Phil. Mag. 14, 271 (1966).
[18]G. Vineyard, J. Phys. Chem. Solids 3, 121 (1957).
[19]T. Heumann and W. Reerink, Acta Met. 14, 201 (1966).
[20]N. Peterson and S. Rothman, Phys. Rev. 154, 558 (1967).
[21]T. Hirone, N. Kunitomi, and M. Sakamoto, J. Phys. Soc. Japan 13, 840 (1958).
[22]M. Wanin and A. Kohn, Compt. Rend. 267, 1558 (1968).
[23]D. Marsh, Tracer Lab JCN, Oakland, Calif. (private communication).
[24]P. Shewmon, *Diffusion in Solids* (McGraw-Hill, New York, 1963), p. 7.
[25]T. Heumann and R. Imm, J. Phys. Chem. Solids 29, 1613 (1968).
[26]F. Buffington, K. Hirano, and M. Cohen, Acta Met. 9, 434 (1961).
[27]C. Wert and C. Zener, Phys. Rev. 76, 1169 (1949).
[28]C. Walter and N. Peterson, Phys. Rev. 178, 922 (1969).
[29]N. Peterson and L. Barr (unpublished).
[30]N. Peterson, Phys. Rev. 136, A568 (1964).
[31]*Diffusion in BCC Metals* (ASM, Metals Park, Ohio, 1965).
[32]J. Mundy and L. Barr, Phil. Mag. 14; 8, 785 (1966).
[33]N. Peterson and S. Rothman, Phys. Rev. 163, 645 (1967).
[34]D. Graham, J. Appl. Phys. 40, 2386 (1969).

PHYSICAL REVIEW B VOLUME 2, NUMBER 6 15 SEPTEMBER 1970

Electron Tunneling Cr-Cr_2O_3-Metal Junctions

G. I. Rochlin and P. K. Hansma*
Department of Physics, University of California, Berkeley, California 94720
and
Inorganic Materials Research Division, Lawrence Radiation Laboratory, Berkeley, California 94720

(Received 16 February 1970)

Conductance measurements on high-quality thin-film Cr-Cr_2O_3-metal tunnel junctions show neither structure due to the antiferromagnetic energy gap of bulk Cr nor zero-bias anomalies. The conductance is almost linear in voltage at low temperatures and biases, with fine structure at 28, 44, 62, and 82 meV. These results are in qualitative agreement with the assumption of inelastic tunneling via elementary excitations of the Cr_2O_3 barrier.

We have measured the temperature and magnetic field dependence of the conductance of more than 80 thin-film Cr-Cr_2O_3-M tunnel junctions, where M (metal) is Ag, Sn, or Pb. In contrast to other reports,[1,2] none of our junctions exhibit giant resistive anomalies. Although the even conductance $G_e(V) \equiv \frac{1}{2}[G(+V)+G(-V)]$ is linear in dc bias V at low temperatures, the temperature and magnetic field dependence indicate that this is not due to impurity-induced zero-bias anomalies[1-3] or small metallic inclusions.[4] In particular, (a) $G(V)$ has no observable magnetic field dependence to $<0.1\%$ for applied magnetic fields (H) between 0 and 30 kG at 1.2 °K; (b) below 4.2 °K, $G(0)$ is nearly temperature independent, having a slope of $\lesssim 0.5\%$ per °K; (c) the shape of $G_e(V)$ is independent of both magnetic field and temperature in the range $1.1 \lesssim T \lesssim 4.2$ °K, $0 \lesssim H \lesssim 30$ kG. When Sn or Pb was used as the second electrode, excellent superconducting tunnel characteristics were observed below T_c; for superconducting Pb electrodes, $G(0)$ at 1.2 °K was as low as $\approx 0.1\%$ of the normal-state conductance, and the phonon structure due to the strong coupling behavior of Pb was as large as in the best Al-I-Pb junctions.[5] We conclude that the electron transfer mechanism is